

Vehicular Teamwork: Collaborative localization of Autonomous Vehicles

Jacob Hartzler and Srikanth Saripalli¹

Abstract—This paper develops a distributed collaborative localization algorithm based on an extended kalman filter. This algorithm incorporates Ultra-Wideband (UWB) measurements for vehicle to vehicle ranging, and shows improvements in localization accuracy where GPS typically falls short. The algorithm was first tested in a newly created open-source simulation environment that emulates various numbers of vehicles and sensors while simultaneously testing multiple localization algorithms. Predicted error distributions for various algorithms are quickly producible using the Monte-Carlo method and optimization techniques within MatLab. The simulation results were validated experimentally in an outdoor, urban environment. Improvements of localization accuracy over a typical extended kalman filter ranged from 2.9% to 9.3% over 180 meter test runs. When GPS was denied, these improvements increased up to 83.3% over a standard kalman filter. In both simulation and experimentally, the DCL algorithm was shown to be a good approximation of a full state filter, while reducing required communication between vehicles. These results are promising in showing the efficacy of adding UWB ranging sensors to cars for collaborative and landmark localization, especially in GPS-denied environments. In the future, additional moving vehicles with additional tags will be tested in other challenging GPS denied environments.

I. INTRODUCTION

Currently, there is significant work being performed to develop autonomous vehicles. Such vehicles have the capacity to reduce risk and increase free time of riders. In the development of autonomous vehicles, a key consideration is reliable localization in order to plan for and react to the environment. Typically, high accuracy position is achieved through the use of a Global Navigation Satellite Systems such as GPS. The use of GPS with an Inertial Measurement Unit (IMU) or odometry measurements can lead to an accurate positioning system [1].

Reliable GPS measurements are often not available. Because GPS receivers must have line of sight with at least four satellites, environments that include obstructions pose significant challenges. Urban canyons, tunnels, or indoor environments degrade or fully obstruct GPS signals, forcing a navigation system to rely on dead reckoning [2]. These measurements are subject to drift, and therefore cannot be trusted after continued interruption of GPS signal. As such, it would be advantageous to the continued development of autonomous vehicles to use an exteroceptive sensor for navigation through environments where GPS is typically denied.

Ultra-Wideband (UWB), defined as radio technology exceeding 500 MHz or 20% of the arithmetic center frequency

[3], utilizes low-energy pulse communication typically for short-range, high-bandwidth applications. By measuring time of flight across various frequencies, it is possible to measure distance between modules while overcoming multipath errors [4]. This has allowed UWB modules to be applied towards localization and tracking problems [5]. With the continued development of UWB technology and roll out in commercial products [6], the use of these sensors in navigation systems should continue to be explored.

There are many examples of using UWB ranging modules for high-accuracy indoor localization of ground or aerial systems. These systems typically measure with respect to fixed landmark anchors [7], [8]. There have been examples of utilizing indoor positioning system simulations and physical experiments to predict and show localization accuracy improvements from incorporating UWB measurements to an extended Kalman filter (EKF) [9], [10]. There are also examples of using UWB modules for outdoor vehicular environments. Such a framework has the capacity to increase localization accuracy of existing systems, or provide accurate localization in environments where GPS is not reliable, such as tunnels or urban canyons, as was shown in [11]. This has applications in the localization of autonomous vehicles using road landmarks [12].

By using UWB, autonomous vehicles can generate ranging estimates to other independent moving vehicles in a process known as collaborative localization. An example of this is shown in [13], where initial experimentation was performed measuring with respect to a fixed vehicle. Given a network of vehicles, it is possible to leverage relative measurements to provide better localization accuracy as a group, than as a collection of individuals. Just like measurements to landmarks, these measurements are not subject to drift when GPS measurements are obscured, and can be made available in both indoor and outdoor environments. These measurements can leverage the growing number of intelligent vehicles on the road, and can increase the accessible area of autonomous vehicles. These collaborative methods can be generally classified in two groups: centralized methods, and decentralized methods.

Centralized collaborative localization (CCL) methods use a single or multiple fusion centers, to which every vehicle communicates measurement information. These state estimators are capable of producing optimal results, and have been used in a number of applications with success [14]. Issues with centralized networks include sensitivity to failure or disconnection, as well as bandwidth and computational power. As the number of measurements made can increase on the order of $\mathcal{O}(n^2)$, centralized networks can meet constraints

¹Jacob Hartzler and Srikanth Saripalli are with the Department of Mechanical Engineering, Texas A&M University, College Station, Texas, USA
jmhartzler@tamu.edu, ssaripalli@tamu.edu

when large networks of nodes are implemented with complex measurements or update functions.

Decentralized collaborative localization (DCL) methods are defined by distributing the state estimation computation across every agent in the network. Unlike centralized methods, DCL methods are not susceptible to single point failures. These approximations of the centralized method can extend the framework to decrease convergence time [15] or computational cost without loss of accuracy [16]. Very promising has been the work in [17] which proposed a CL framework that tracks correlations while limiting communication to the two robots that obtain a relative measurement. The algorithm is recursive, reducing memory requirements and it supports generic measurement models, and was implemented using the UTIAS data set, which uses cameras for relative bearing and ranging [18].

This paper seeks to expand upon these previous works with an open-sourced simulation framework for testing and validating the DCL algorithm in various scenarios with the Monte-Carlo method. It is with this simulation environment that this paper seeks to validate the efficacy of the DCL algorithm compared to a full state Kalman filter. Additionally, this paper presents experimental results showing improvement of localization accuracy for a vehicle in an urban environment when using the DCL algorithm.

II. DECENTRALIZED COLLABORATIVE LOCALIZATION

The decentralized collaborative localization algorithm, developed by Luft et. al. [17] and reproduced in Algorithms 1 to 3, is a form of a Kalman filter that approximates the centralized filter through distributed computation. The estimation of the entire state of a network is broken down into smaller filters where each vehicle has private controls and measurements that are used internally and relative measurements that require the sharing of state and covariance information.

For a network of N vehicles, let X_i be the 6-DOF state of vehicle i such that $X_i = [x, y, \theta, \dot{x}, \dot{y}, \dot{\theta}]$. Each vehicle has an estimate at time t of its state \hat{X}_i^t and covariance Σ_{ii}^t . The joint state estimate of the vehicle network is $\hat{X}^t = [\hat{x}_1^t; \dots; \hat{x}_N^t]$ and the joint covariance is $\Sigma^t = [\Sigma_{ij}^t]_{i,j \in \{1, \dots, N\}}$. With this network, a decentralized collaborative localization filter can be used.

A. Initialization

It is assumed upon initialization the vehicle states are uncorrelated. Therefore, the network state can be initialized with the initial estimates \hat{X}_i of each vehicle and the cross correlation terms set to zero.

$$\{\Sigma_{ij}^t = 0\}_{i,j \in \{1, \dots, N\} | i \neq j} \quad (1)$$

When the vehicles come into sensing range, generally the cross correlation $\Sigma_{ij}^{t+1} \neq 0$ and therefore the cross-correlation term can be decomposed according to [19].

$$\Sigma_{ij}^{t+1} = \sigma_{ij}^{t+1} (\sigma_{ji}^{t+1})^T \quad (2)$$

where the simple decomposition $\sigma_{ij}^{t+1} = \Sigma_{ij}^{t+1}$ and $\sigma_{ji}^{t+1} = \mathbb{I}$ is chosen.

B. Prediction

It is assumed that the vehicles follow the motion model f with process noise R and control input u which in this case is an IMU measurement. The prediction step for vehicle i is given by the standard EKF equations in Algorithm 1 with the addition of applying the linearized motion model to update the decomposed cross correlation terms σ_{ij} .

Algorithm 1: Prediction for Vehicle i

Input: $\hat{X}_i^t, \Sigma_{ii}^t, \{\sigma_{ij}^t\}_{j \in \{1, \dots, N\} \setminus \{i\}}, u$
Output: $\hat{X}_i^{t+1}, \Sigma_{ii}^{t+1}, \{\sigma_{ij}^{t+1}\}_{j \in \{1, \dots, N\} \setminus \{i\}}$
 $F = \frac{\partial f(X, u)}{\partial X}(\hat{X}_i^t, u)$
 $\hat{x}_i^{t+1} = f(\hat{x}_i^t, u)$
 $\Sigma_{ii}^{t+1} = F \Sigma_{ii}^t F^T + R$
for $j \in \{1, \dots, N\} \setminus \{i\}$ **do**
 $\sigma_{ij}^{t+1} = F \sigma_{ij}^t$

C. Private Update

It is assumed that the private update measurements are functions of the state of a single vehicle with a Gaussian error disturbance.

$$z_i^t = h(\hat{x}_i^t) + \nu_p \quad (3)$$

with $\nu_p \sim \mathcal{N}(0, R_i^t)$, R_i^t being the measurement noise, and g being the measurement model. The private update step for the system is shown in Algorithm 2. Again, the algorithm is very similar to the typical update step of an EKF with the addition of updates to the decomposed cross correlation terms.

Algorithm 2: Private Update for Vehicle i

Input: $\hat{X}_i^t, \Sigma_{ii}^t, \{\sigma_{ij}^t\}_{j \in \{1, \dots, N\} \setminus \{i\}}, z$
Output: $\hat{X}_i^{t+1}, \Sigma_{ii}^{t+1}, \{\sigma_{ij}^{t+1}\}_{j \in \{1, \dots, N\} \setminus \{i\}}$
 $H = \frac{\partial h(X)}{\partial X}(\hat{X}_i^t)$
 $K_i = \Sigma_{ii}^t H^T (H \Sigma_{ii}^t H^T + Q)^{-1}$
 $\hat{X}_i^{t+1} = \hat{X}_i^t + K_i [z - h(\hat{X}_i^t)]$
 $\Sigma_{ii}^{t+1} = (\mathbb{I} - K_i H) \Sigma_{ii}^t$
for $j \in \{1, \dots, N\} \setminus \{i\}$ **do**
 $\sigma_{ij}^{t+1} = (\mathbb{I} - K_i H) \sigma_{ij}^t$

D. Relative Update

Lastly, it is assumed that the relative update measurement is a function of the state of two vehicles i and j , with a Gaussian error disturbance.

$$z_i^t = g(\hat{x}_i^t, \hat{x}_j^t) + \nu_p \quad (4)$$

with $\nu_p \sim \mathcal{N}(0, R_i^t)$, R_i^t being the measurement noise, and g being the measurement model. These updates come from vehicle-to-vehicle relative UWB ranging measurements. The relative update step for the system is shown in Algorithm 3. The update contains updates to the state estimates and covariances of the two vehicles involved in the relative measurement by combining the decomposed cross correlation terms. As explained in [17], the inability to simplify the cross correlation update equation for all non-involved vehicles k into the form

$$\sigma_{ab}^{t+1} = A\sigma_{ab}^t \mid a \in \{i, j\}, b \in \{1, \dots, N\} \setminus \{i, j\} \quad (5)$$

creates difficulty when trying to minimize necessary communication between vehicles. The update equation used is not only stable, but also also a very good approximation, as will be shown in simulation.

Algorithm 3: Relative Update for Vehicles i, j

Input: $\hat{X}_i^t, \Sigma_{ii}^t, \{\sigma_{ij}^t\}_{j \in \{1, \dots, N\} \setminus \{i\}}$, r

Output: $\hat{X}_i^{t+1}, \Sigma_{ii}^{t+1}, \{\sigma_{ij}^{t+1}\}_{j \in \{1, \dots, N\} \setminus \{i\}}$

if vehicle i detects vehicle j **then**

receive from vehicle j : $\hat{X}_j^t, \Sigma_{jj}^t, \sigma_{ji}^t$

$\Sigma_{ij}^t = \sigma_{ij}^t (\sigma_{ji}^t)^T$

$\Sigma_{aa}^t = \begin{bmatrix} \Sigma_{ii}^t & \Sigma_{ij}^t \\ (\Sigma_{ij}^t)^T & \Sigma_{jj}^t \end{bmatrix}$

$H_a = \begin{bmatrix} \frac{\partial h(X_i, X_j)}{\partial X_i}(\hat{X}_i^t, \hat{X}_j^t), & \frac{\partial h(X_i, X_j)}{\partial X_j}(\hat{X}_i^t, \hat{X}_j^t) \end{bmatrix}$

$K_a = \Sigma_{aa}^t H_a^T (H_a \Sigma_{aa}^t H_a^T + Q)^{-1}$

$\begin{bmatrix} \hat{X}_i^{t+1} \\ \hat{X}_j^{t+1} \end{bmatrix} = \begin{bmatrix} \hat{X}_i^t \\ \hat{X}_j^t \end{bmatrix} + K_a [r - h(\hat{X}_i^t, \hat{X}_j^t)]$

$\begin{bmatrix} \Sigma_{ii}^t & \Sigma_{ij}^t \\ (\Sigma_{ij}^t)^T & \Sigma_{jj}^t \end{bmatrix} = (\mathbb{I} - K_a H) \Sigma_{aa}^t$

send to vehicle j : $\hat{X}_j^{t+1}, \Sigma_{jj}^{t+1}$

$\sigma_{ij}^{t+1} = \Sigma_{ij}^{t+1}$

for $k \in \{1, \dots, N\} \setminus \{i, j\}$ **do**

$\sigma_{ik}^{t+1} = \Sigma_{ii}^{t+1} (\Sigma_{ii}^t)^{-1} \sigma_{ik}^t$

if vehicle j is detected by vehicle i **then**

send to vehicle i : $\hat{X}_j^t, \Sigma_{jj}^t, \sigma_{ji}^t$

receive from vehicle i : $\hat{X}_i^{t+1}, \Sigma_{ii}^{t+1}$

$\sigma_{ij}^{t+1} = \mathbb{I}$

for $k \in \{1, \dots, N\} \setminus \{i, j\}$ **do**

$\sigma_{jk}^{t+1} = \Sigma_{jj}^{t+1} (\Sigma_{jj}^t)^{-1} \sigma_{jk}^t$

III. SIMULATION DESIGN

In order to simulate the efficacy of the collaborative localization algorithm, an open-source simulation framework that would be flexible in the number of cars and their

positions was created in MatLab [20]. This simulation included sensing models for IMU, wheel odometry, GPS, and UWB measurements between both stationary and moving landmarks. The simulation was vectorized and parallelized to greatly increase processing speed for large Monte-Carlo simulations, and allows for error distributions to be quickly estimated given any vehicle scenario. Lastly, multiple localization algorithms can be run in parallel to directly compare performance of each with the same set of random sensor measurements. This, combined with the ability to simultaneous simulation thousands of experiments, allows for direct comparisons of error distributions.

A. Sensing Models

The sensing error models used in the simulation all took the form of zero-mean Gaussian distributions.

$$z = h(\hat{x}) + \nu \quad (6)$$

With there exist better models for the various sensors used, this assumption allows for sufficient testing of the various algorithms, without sacrificing speed due to computational complexity. Specifically, there is significant computational advantage in generating large vectors of normally distributed random numbers, and this advantage is what was leveraged to make the Monte-Carlo simulation run on the order of minutes rather than hours.

B. Simulation Output

The resulting output of this software package is the RMS error of position and heading for each simulated vehicle for every simulation run. The number of simulations run can range from a single evaluation to up to 100,000 runs, depending on system memory. These results can be plot as a distribution of errors for comparing various parallel localization algorithms. When compiled in such Monte Carlo simulations, these data can be used to evaluate filter performance improvements.

IV. SIMULATION RESULTS

Using the simulation framework, it was possible to test a wide variety of vehicle environments and sensor configurations. These configurations, with an example shown in Fig. 1, included vehicles moving parallel to each other, vehicles moving perpendicular in street crossings, and moving in groups in tunnels without GPS measurements but with UWB landmarks. Additionally, it was possible to add stationary UWB landmarks to each of these situations.

In each of the three different scenarios, three different localization algorithms were tested: Extended Kalman Filter (EKF), Centralized Collaborative Localization (CKF), and Decentralized Collaborative Localization (DCL). Note that the CCL algorithm is a full-state EKF that receives every sensor message and maintains a single state estimate for all vehicles. The CCL algorithm represents the theoretical maximal performance of a DCL algorithm, and is therefore a good test of the assumptions made and check for overconfidence.

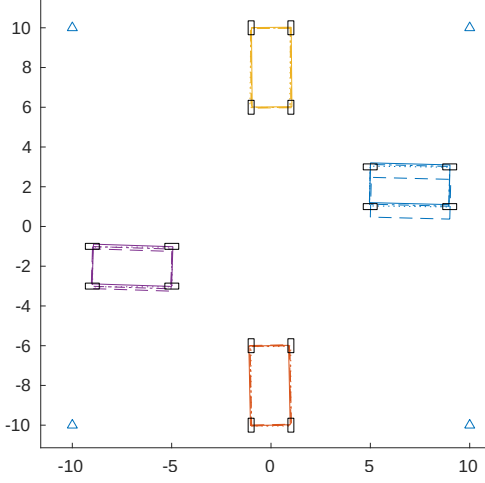


Fig. 1. Street crossing example of using the simulation with multiple parallel localization algorithms

The resulting error distributions from the Monte Carlo simulations performed are shown in Figs. 2 to 4. These figures show position localization accuracy of three algorithms run in parallel in each of the simulated scenarios. A numerical summary of the simulation results is shown in Table I.

These simulations showed that collaborative UWB measurements offered improvements to localization accuracy across all experiments. As would be expected, using more vehicles improved accuracy, and using stationary landmarks also offered significant improvements. This was especially the case in situations where GPS data was not available such as in a tunnel environment.

Additionally, it should be noted the CCL and DCL algorithms performed, on average, within 1 cm of accuracy between each other across the simulation scenarios. While this research originally sought to improve the update equation approximation made in the DCL algorithm, this result helps to validate this method for very closely approximate a centralized Kalman Filter without requiring large amounts of communication between vehicles. Additionally, these simulations also validate the update equation approximation does not result in overconfidence of the filter, as divergence was not seen in any of the hundreds of thousands of simulated experiments.

Therefore, the simulations validated the DCL algorithm for its use in collaborative localization of autonomous vehicles and that the approximation to decentralize the filter did not induce a noticeable reduction in accuracy.

V. EXPERIMENTAL RESULTS

The filter framework was tested in downtown Bryan, Texas using the Unmanned Systems Lab autonomous trolley shown in Fig. 5. The Decwave EVK1000 UWB ranging evaluation boards were mounted alongside a VectorNav VN-300 INS. The trolley itself includes PACMod, a by-wire kit prepared

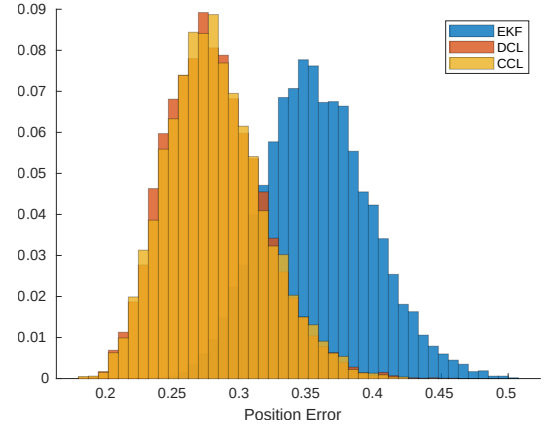


Fig. 2. Monte Carlo Simulation with 10,000 runs of two collaborative vehicles moving in parallel

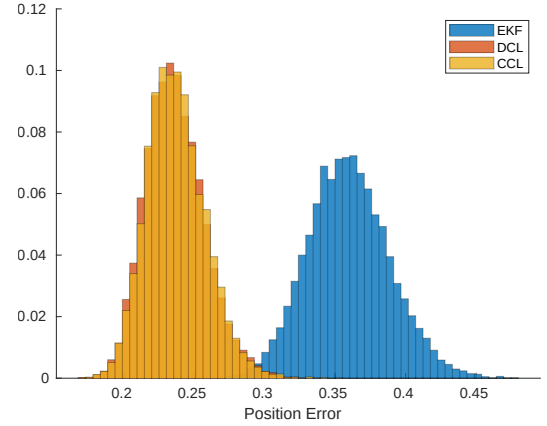


Fig. 3. Monte Carlo Simulation with 10,000 runs of two collaborative vehicles moving in parallel with landmarks every 50 meters

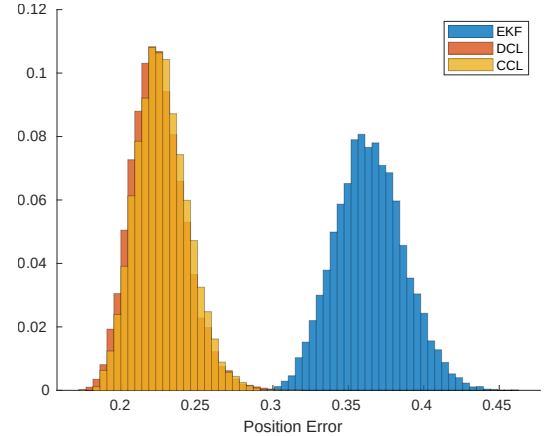


Fig. 4. Monte Carlo Simulation with 10,000 runs of two collaborative vehicles moving in parallel with landmarks every 50 meters

Simulation	GPS	EKF	DCL	CCL
Parallel	Yes	0.19	0.15	0.15
Crossing	Yes	0.19	0.13	0.13
Tunnel	No	0.19	0.12	0.12

TABLE I

SUMMARY OF MONTE-CARLO SIMULATION RMS POSITION ERRORS, IN METERS



Fig. 5. Unmanned Systems Lab Autonomous Trolley

by Autonomous Stuff, which gives access to wheel odometry and steering angle measurements. These sensors formed the basis of the filters, while a secondary real-time kinematic GPS (RTK GPS) system from ArduSimple was used as ground truth for filter performance evaluation as it can obtain accuracy to 2 cm.

Using tripods, additional UWB ranging modules were placed in various experimental setups to either represent stationary landmarks or non-stationary vehicles. Due to limitations of in-person testing, only one moving vehicle was used and other tags were simulated as vehicles using a steady state covariance derived from the trolley at rest for a long period of time. Due to the nature of the UWB modules making available all measurements, a vehicle-to-vehicle network was not necessary in order to run any of the three algorithms on a single trolley's computer. The Robot Operating System (ROS) middleware was used to make available the sensor measurements as well as run the separate localization algorithms.

Using this setup, the simulated environment was recreated experimentally in the three different configurations listed and RMS position errors over the course of 180 meter runs were calculated with respect to the on board RTK GPS.

As in the simulations, the addition of the UWB sensors on the vehicle offered improvements to the localization accuracy of the vehicle in all scenarios. This improvement was even more pronounced when GPS data was not available in the tunnel scenario. A summary of the results are shown in Table II. The DCL algorithm, again, performed as well as the CCL algorithm, down to 1 cm. This further validates the approximations made led to accurate yet not overconfident updates to cross correlation covariance matrices.

Interestingly, despite using the same intrinsic sensor errors in simulation, the experimental errors were significantly higher. It is believed that this occurred due to poor GPS signal in the testing environment. Despite this, relative improvements were still seen due to the addition of UWB measurements and collaborative localization. These improvements, as expected, were lower when GPS was available, producing improvements of 2.9% and 9.3% for the Parallel and Crossing scenarios respectively. However, without GPS, the system was subject to drift and therefore saw significant

improvements when adding UWB: 83.3% improvement in the tunnel scenario.

Therefore, in all cases, experimentation showed the addition of UWB ranging to other vehicles led to improvements in localization accuracy, with the most significant improvements seen when GPS was unavailable.

Experiment	GPS	EKF	DCL	CEKF
Parallel	Yes	2.06	1.81	1.81
Crossing	Yes	2.32	1.61	1.61
Tunnel	No	7.78	1.30	1.30

TABLE II

SUMMARY OF EXPERIMENTAL RMS POSITION ERRORS, IN METERS, OVER A DISTANCE OF 180 METERS

VI. FUTURE WORK

In the future, testing will include more in-person experiments with multiple moving vehicles and a greater number of UWB tags. This would allow for better evaluation of truly cooperative localization of vehicles using UWB and will further validate the algorithm used in simulation. This will also explore the use of real-time varying covariance estimations in the update equations and any issues with measurement delays and networking between vehicles. Additionally, transitioning into GPS-denied environments will be explored such as vehicles entering tunnels or warehouses, and how the use of stationary UWB landmarks can aid in navigating these challenging environments.

VII. CONCLUSIONS

In conclusion, this paper presented the creation of an open-source collaborative localization simulation package as well simulated and experimental results of collaborative localization of autonomous vehicles. The simulation is capable of handling user defined scenarios with multiple vehicles, and can quickly create error distributions using the Monte-Carlo method and optimization techniques within MatLab.

In both simulations and in experiments, this work validated the DCL algorithm is a very good approximation of a full state CCL algorithm, while significantly reducing the amount of communication required between vehicles. Additionally, it was shown in simulation and experimentally the inclusion of collaborative localization improved the localization accuracy of autonomous vehicles, especially when in environments without GPS measurements available. Improvements in localization accuracy of 2.9% and 9.3% were shown when vehicles were moving in parallel and through an intersection, respectively. While vehicles were moving in a simulated tunnel environment without GPS, the improvement due to collaboration was 83.3%.

Therefore, methods of collaborative localization show promise for increasing localization accuracy of autonomous vehicles, especially in applications where GPS data is not readily available. UWB ranging is a viable way to include these types of measurements, and its application

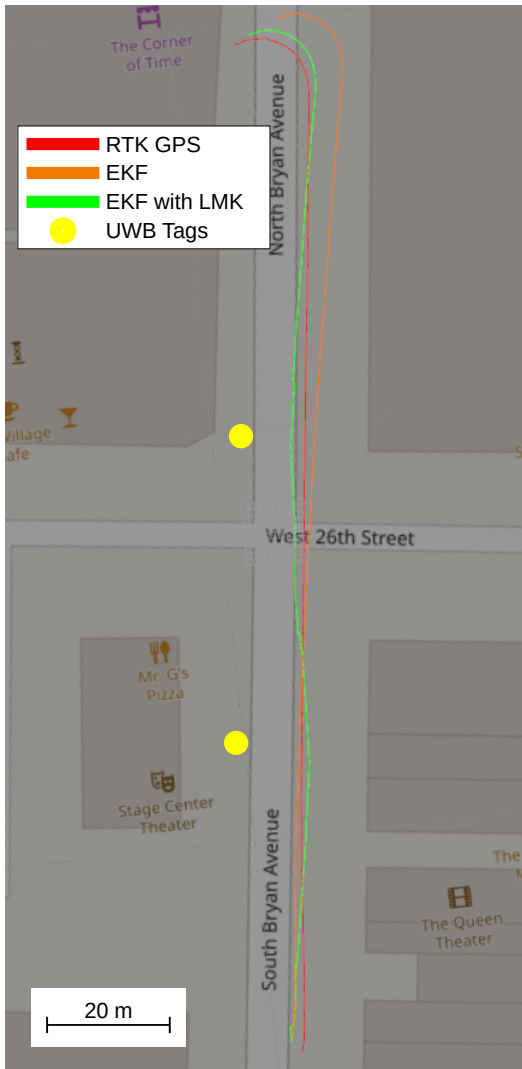


Fig. 6. Experimental results of DCL algorithm in tunnel scenario

will continue to be explored with increased numbers of measurements as well as applications to other challenging environments.

REFERENCES

- [1] K. Bimbray, "Autonomous cars: Past, present and future - a review of the developments in the last century, the present scenario and the expected future of autonomous vehicle technology," *ICINCO 2015 - 12th International Conference on Informatics in Control, Automation and Robotics, Proceedings*, vol. 1, pp. 191–198, 01 2015.
- [2] G. Balamurugan, V. Jayaraman, and D. V. Naidu, "Survey on uav navigation in gps denied environments," in *2016 International conference on Signal Processing, Communication, Power and Embedded System (SCOPEs)*, 10 2016, pp. 198–204.
- [3] The ITU Radiocommunication Assembly, "Characteristics of ultra-wideband technology," Federal Communication Commission, Standard, 2006.
- [4] M. Aftanas, J. Rovnakova, M. Drutarovsky, and D. Kocur, "Efficient method of toa estimation for through wall imaging by uwb radar," in *2008 IEEE International Conference on Ultra-Wideband*, vol. 2, 2008, pp. 101–104.
- [5] Y. Zhou, C. Law, and J. Xia, "Ultra low-power uwb-rfid system for precise location-aware applications," in *Wireless Communications and Networking Conference Workshops (WCNCW)*, 04 2012.
- [6] Apple, "Iphone 11: Share. find. play. more precisely than ever." 2020.

- [7] G. Fan and Y. Sun, "An improved ins/pdr/uwb integrated positioning method for indoor foot-mounted pedestrians," *Sensor Review*, vol. 39, 11 2018.
- [8] S. Sun, J. Hu, J. Li, R. Liu, M. Shu, and Y. Yang, "An ins-uwb based collision avoidance system for agv," *Algorithms*, vol. 12, p. 40, 02 2019.
- [9] L. Yao, Y. A. Wu, L. Yao, and Z. Z. Liao, "An integrated imu and uwb sensor based indoor positioning system," in *2017 International Conference on Indoor Positioning and Indoor Navigation (IPIN)*, 2017, pp. 1–8.
- [10] A. Benini, A. Mancini, and S. Longhi, "An imu/uwb/vision-based extended kalman filter for mini-uav localization in indoor environment using 802.15.4a wireless sensor network," *Journal of Intelligent & Robotic Systems*, vol. 70, 04 2013.
- [11] K. Dierenbach, S. Ostrowski, G. Józków, C. Toth, D. Grejner-Brzezinska, and Z. Koppanyi, "Uwb for navigation in gnss compromised environments," in *28th International Technical Meeting of the Satellite Division of The Institute of Navigation (ION GNSS+ 2015)*, 08 2015.
- [12] J. S. Martín, A. Cortés, L. Zamora-Cadenas, and B. J. Svensson, "Precise positioning of autonomous vehicles combining uwb ranging estimations with on-board sensors," *Journal of Intelligent & Robotic Systems*, vol. 9, p. 1238, 09 2020.
- [13] E. Ghanem, K. O'Keefe, and R. Klukas, "Estimating vehicle-to-vehicle relative position and attitude using multiple uwb ranges," *International Conference on Indoor Positioning and Indoor Navigation - Work-in-Progress Papers*, 2019.
- [14] A. Howard, M. J. Matark, and G. S. Sukhatme, "Localization for mobile robot teams using maximum likelihood estimation," in *IEEE/RSJ International Conference on Intelligent Robots and Systems*, vol. 1, 2002, pp. 434–439.
- [15] F. R. Fabresse, F. Caballero, and A. Ollero, "Decentralized simultaneous localization and mapping for multiple aerial vehicles using range-only sensors," in *2015 IEEE International Conference on Robotics and Automation (ICRA)*, 2015, pp. 6408–6414.
- [16] A. Howard, M. J. Mataric, and G. S. Sukhatme, "Putting the 'i' in 'team': an ego-centric approach to cooperative localization," in *2003 IEEE International Conference on Robotics and Automation (Cat. No.03CH37422)*, vol. 1, 2003, pp. 868–874 vol.1.
- [17] L. Luft, T. Schubert, S. I. Roumeliotis, and W. Burgard, "Recursive decentralized localization for multi-robot systems with asynchronous pairwise communication," *The International Journal of Robotics Research*, vol. 37, no. 10, pp. 1152–1167, 2018.
- [18] K. Y. Leung, Y. Halpern, T. D. Barfoot, and H. H. Liu, "The utias multi-robot cooperative localization and mapping dataset," *The International Journal of Robotics Research*, vol. 30, no. 8, p. 969–974, 2011.
- [19] S. I. Roumeliotis and G. A. Bekey, "Distributed multirobot localization," *IEEE Transactions on Robotics and Automation*, vol. 18, no. 5, pp. 781–795, 2002.
- [20] J. Hartzler, "collab.localization: A repository of simulation and experimental work in decentralized collaborative localization," <https://github.com/unmannedlab/collab.localization>, 2021, v0.1-beta.